Assist-As-Needed Electromyography-based Control for a Wearable Ankle Robotic Orthosis*

Luís Moreira, Joana Figueiredo, João Cerqueira, and Cristina P. Santos

***Abstract*— The challenge of addressing the critical public health issue of lower limb disability has led to the exploration of robotic assistive devices for rehabilitation, as a complement to conventional therapies. However, achieving optimal synergy between robotic activity and human effort remains a persistent challenge. Even the optimal control of Assist-as-Needed (AAN) remains to be solved. This study addresses this challenge by proposing an AAN electromyography (EMG)-based control strategy to automatically assist the walking motion throughout the entire gait cycle. The AAN EMG-based control strategy was integrated into an active orthosis to provide automatic ankle assistance. Preliminary results from a healthy male participant demonstrate that the ankle orthosis increased its plantar flexion assistance by 28% when the user's ankle joint torque decreased by 6% and his EMG signals from Gastrocnemius Lateralis and Tibialis Anterior decreased by 41% and 29%, respectively. In addition, the results show that the ankle orthosis was able to perform the gait pattern when there was no user participation, demonstrating the system's AAN capacity.**

I. Introduction

Restoring the walking ability of people with lower limb impairments is crucial, as it empowers them to regain independence in performing their daily tasks. Current directions in rehabilitation point to the incorporation of robotic assistive devices, such as active orthoses and exoskeletons, alongside conventional physiotherapy. These devices are designed to work hand-in-hand with traditional methods, aiming to enhance the coordination of movements and muscle function in individuals facing challenges with motor abilities [1]. Therefore, trajectory tracking controls, such as position control strategies, have been extensively employed [2], [3]. However, as indicated in [2], despite the repetitive nature of gait training imposed by these control strategies, they tend to ignore the human-robot interaction and, consequently, the needs of each user. As a result, these strategies may limit motor relearning and end up being abandoned [3], [4].

In the last years, electromyography (EMG)-based torque control strategies have been suggested to promote a smoother use of robotic assistive devices [5]. At this level, various EMG-based torque control strategies, typically based on a threshold [6], proportional [7], or Hill-type muscle model approaches [8], were proposed to foster the patient's participation while wearing robotic assistive devices. In EMG-based torque controls based on threshold methods, also known as EMG-triggered controllers, the assistance of the assistive device is triggered when EMG signals achieve certain threshold values. Apart from the intra- and inter-subject threshold dependence, this method does not allow continuous control to be achieved, as it only provides assistance when the threshold values are reached [9]. To solve that, both proportional controls and those based on Hill-type models have been proposed by building linear and non-linear models, respectively, by correlating EMG signals with joint torques [7], [8], [10]. While in the proportional control, the amount of gain required is found by trial-and-error experiments, which may result in an inaccurate control, the Hill-type models (i) depend on muscle-specific parameters that are difficult to measure; (ii) present numerical instability issues; and (iii) are time-consuming, which may hinder their real-time application [8], [11]. Additionally, despite being a valuable contribution to muscle strengthening, these EMG-based torque controls do not consider different levels of motor disabilities, not assisting the user when and as much as needed [12].

Assist-As-Needed (AAN) EMG-based control strategies have been proposed to provide the robotic assistance required for users to complete a motion while considering their motor disabilities and invoking their participation [4], [9], [12]–[18]. For that, torque control loops are adopted, in which the user's joint torque is commonly estimated based on EMG signals, while reference joint torques are set according to assistance ratios [4], [9], [12]–[18]. Nonetheless, most of the already proposed AAN EMG-based control strategies (i) were developed for upper limbs [12]–[14]; (ii) depend on Hill-type models to estimate the user's joint torque, which may result in complex, user-dependent calibration, and time-consuming methods [4], [15]–[18]; (iii) are not adaptable since they rely on fixed assistance ratios to define the desired joint torque trajectories [4], [15], [16]; and (iv) were not developed to assist the walking motion, but rather focus on flexion and extension movements of the lower limb joints [4], [9], [16]–[18].

This study tackles the above-mentioned limitations by proposing an AAN EMG-based control strategy to

*This work was funded by the Fundação para a Ciência e Tecnologia (FCT) under the scholarship reference 2020.05711.BD, with the FAIR project under grant 2022.05844.PTDC, under the Stimulus of Scientific Employment with the grant 2020.03393.CEECIND, under the national support to R&D units grant through the reference project UIDB/04436/2020 and UIDP/04436/2020.

Luís Moreira is with the Center for MicroElectroMechanical Systems (CMEMS), University of Minho, 4800-058 Guimarães, Portugal.

Joana Figueiredo is with the CMEMS, University of Minho, 4800-058 Guimarães, Portugal and with LABBELS - Associate Laboratory, Braga/Guimarães, Portugal (e-mail: joana.figueiredo@dei.uminho.pt).

João Cerqueira is with the Life and Health Sciences Research Institute (ICVS), University of Minho, 4800-058 Guimarães, Portugal and with Clinical Academic Center (2CA-Braga), Hospital of Braga, 4700-099 Braga, Portugal.

Cristina P. Santos is with CMEMS, University of Minho, 4800-058 Guimarães, Portugal, and with the LABBELS - Associate Laboratory, 4800-058 Guimarães, Portugal and with the 2CA-Braga, Hospital of Braga, 4700-099 Braga, Portugal.

automatically assist the walking motion throughout the entire gait cycle. The system implements an outer loop torque control and an inner loop position control, which adapts the level of assistance to be provided to the user in real-time and automatically. To do this, the system compares the user's participation (through the ankle torque trajectory estimated by a Deep Learning (DL) regressor fed by a fusion of kinematic, EMG, anthropometric, and demographic data [19]) with the user-oriented torque reference trajectory (generated by a DL regressor based on the user's body height and gait speed [20]). The control strategy was designed and implemented into a robotic assistive device (SmartOs - Smart Active Orthotic System [21]) to assist the ankle joint. We present a proof-of-concept to show how the system automatically adapts its assistance in real-time while considering the user's engagement.

II. Materials and Methods

A. SmartOs Description

The SmartOs system, depicted in Fig. 1, employs a non-centralized architecture, structured as a modular and hierarchical framework, being organized into high-, mid-, and low-levels, as proposed in [22]. The main blocks of the framework consist of (i) an Android application; (ii) a Central Control Unit (CCU); (iii) two development boards; (iv) an ankle orthosis; and (v) a power supply. To enhance user comfort and practicality, all these hardware components are combined within a backpack housing the system.

The system is configured through the Android application, defining the user's parameters, assistive control strategies, walking speed, gait analysis tools, and sensor systems to use. The CCU, running the high-level controls at 100 Hz, is implemented using a UDOO X86 computer (2.24 GHz and a Random Access Memory with 4.0 GB). The two boards correspond to STM32F4-Discovery boards (STMicroelectronics, Switzerland). They communicate with the CCU through a UART interface. These development boards comprehend (i) a Wearable Motion LAB, which facilitates real-time data acquisition from sensor systems developed by the team [23], [24] and from external sensors [25]; and (ii) a Low-Level Orthotic System, handling mid- and low-level controllers and interfacing with the right ankle orthosis (Exo-H2, by Technaid, Madrid, Spain [26]), through the Control Area Network (CAN) protocol. The ankle orthosis comprises an electric actuator (EC60 100W Flat Brushless, Maxon, Germany) coupled to a gearbox (CSD-20-160-2A-GR, Harmonic Drive, Japan) with a ratio of 160:1. This setup can deliver an average torque of 35 N.m and a peak torque of 180 N.m [26]. The power supply system is equipped with a lithium iron phosphate battery (LifePO4) of 22.4 V and a hardware interface to power the CCU at 12 V and all development boards at 5 V.

B. EMG Delsys System Integration

For developing an AAN EMG-based control strategy, we integrated the 8-channel Delsys Trigno wireless EMG system (Delsys, MA, USA) into the SmartOs framework (Fig. 1) to measure and record muscle activity during gait. The integration was achieved using the Trigno SDK, enabling real-time acquisition of rectified EMG signals during orthosis use [20].

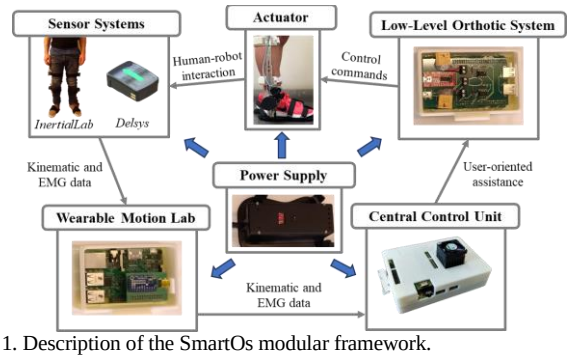

Fig. 1. Description of the SmartOs modular framework.

Further, we developed an algorithm capable of determining, in real-time, the value of maximum voluntary contraction (MVC) per muscle. This MVC value represents the maximum strength production capacity of a muscle and it is used in the AAN EMG-based control to normalize all EMG signals of a muscle by the corresponding maximum [27]. This algorithm should be robust to peaks created due to external perturbations or a momentary displacement of the EMG sensor on the skin. In both cases, momentary peaks with high magnitude and short duration are generated. To avoid this, following the completion of an MVC trial for each muscle, we implemented the following algorithm. First, it identified the maximum value within that trial. Subsequently, two windows are established around that maximum: a vertical window and a horizontal window. The horizontal window spans a maximum of 300 samples. This window includes 150 EMG samples before and after the position of the maximum and between the maximum EMG value recorded and this maximum value subtracted by a threshold value. The threshold value used was 0.0001 V and it was found empirically. Then, for each window, the average of its values is computed. If the average of the horizontal window exceeds the one of the vertical window, this indicates the presence of a disturbance. Thus, the initially identified maximum value is deemed unreliable and discarded. Conversely, if the average of the horizontal window is less than or equal to the average of the vertical window, the MVC value is considered valid and retained. Once the entire MVC trial has been analyzed, the MVC algorithm retains the highest value corresponding to the average value of the horizontal window.

C. AAN EMG-based Control Strategy

The AAN EMG-based control proposed in this work follows a hierarchical control organized into high-, mid-, and low-levels, as depicted in Fig. 2. It combines a torque outer loop and a position inner loop control. In this approach, the outer loop introduces a "softening" effect in the behavior of human-robot interaction, while the inner loop enhances joint stiffness. This helps suppress undesirable disturbances, eliminating the necessity for compensation based on anticipatory control models [3].

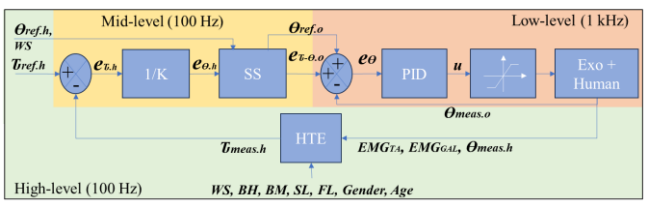

Fig. 2. AAN EMG-based torque control, combining a torque outer loop with a position inner loop. $\tau_{ref.h}$ and $\tau_{meas.h}$ are the human ankle joint reference and

measured torques, respectively. $e_{\tau.h}$ is the human torque error between $\tau_{ref.h}$ and $\tau_{meas.h}$. $e_{\Theta.h}$ is the human position error corresponding to $e_{\tau.h}$. $\Theta_{ref.h}$ and $\Theta_{ref.o}$ are the human and orthosis ankle joint reference angles, respectively. $\Theta_{meas.o}$ is the orthosis ankle joint measured angle. $e_{\tau\text{-}\Theta.o}$ is the orthosis position error corresponding to the $e_{\Theta.h}$. u is the PID command. EMG_{TA} and EMG_{GAL} are the EMG measured from the *Tibialis Anterior* and *Gastrocnemius Lateralis* muscles, respectively. $\Theta_{meas.h}$ is the human hip joint measured angle. *WS* is the walking speed. *BH* and *BM* are the human body height and mass, respectively. *SL* and *FL* are the shank and foot lengths, respectively. *K* is a fixed factor equal to 20. *SS* is a speed scaling block achieved by (1). *PID* is a Proportional-Integral-Derivative (PID) controller. *HTE* is a Human-Torque Estimation (HTE) block.

The high-level controller, implemented at 100 Hz, is responsible for (i) defining the Human ankle joint reference angle ($\Theta_{ref.h}$) and torque trajectories ($\tau_{ref.h}$); and (ii) estimating the Human ankle joint torque trajectory ($\tau_{meas.h}$), in real-time, through the Human-Torque Estimation (HTE) block. The $\Theta_{ref.h}$ is generated by a regression model proposed in [28], considering the user's body height and walking speed. The Convolutional Neural Network (CNN) explored in [19] sets the $\tau_{ref.h}$, according to the $\Theta_{ref.h}$ and its derivatives (angular velocity and angular acceleration), walking speed, anthropometric (body height and mass, shank, and foot lengths), and demographic (gender and age) data. The HTE block is implemented through another CNN detailed in [20]. It estimates the $\tau_{meas.h}$ in less than 2 ms, considering the EMG signals from the *Tibialis Anterior* and *Gastrocnemius Lateralis* muscles (normalized by the corresponding MVCs), hip joint kinematics, walking speed, anthropometric (body height and mass, shank, and foot lengths), and demographic (gender, age) data.

In the mid-level controller, which operates at 100 Hz, the $\tau_{ref.h}$ and $\tau_{meas.h}$ are compared, generating the Human torque error ($e_{\tau.h}$). The $e_{\tau.h}$ is converted into a human position error ($e_{\Theta.h}$) through a fixed scaling value *K* set at 20. This value was empirically found for the used ankle orthosis. Moreover, the mid-level controller defines the (i) orthosis ankle joint reference angle ($\Theta_{ref.o}$) based on the $\Theta_{ref.h}$; and (ii) orthosis position error ($e_{\tau\text{-}\Theta.h}$) that corresponds to the $e_{\Theta.h}$. Both definitions will enable to scale the $\Theta_{ref.o}$ and $e_{\tau\text{-}\Theta.h}$ to the low-level control frequency given the current walking speed, through the empirical equation (1) found in [29].

$$Speed\ Scaling = -34.62 \times Walking\ Speed + 107.32 \quad (1)$$

At the low-level controller (working at 1 kHz), we empirically verified that was required to apply a feedforward position control to prevent the ankle orthosis from moving to positions that could cause injury to the user. This feedforward position control was also proposed in a study [3] to improve trajectory tracking. To this end, a feedforward position control was applied to the inner loop, adding the $\Theta_{ref.o}$ that the orthosis should move to while taking into account the $\tau_{ref.h}$ of the outer loop. The $e_{\tau\text{-}\Theta.h}$, $\Theta_{ref.o}$, and the orthosis ankle joint measured angle ($\Theta_{meas.o}$) are compared, generating the orthosis position error (e_{Θ}), fed to the Proportional-Integral-Derivative (PID) controller. The PID controller was implemented using proportional, integral, and derivative gains of 95, 1.5, and 1.5, respectively. Considering the e_{Θ}, the PID controller computes a PID command (u) that is limited to maximum and minimum values of 2500 and -2500, through a saturator. This command is interpreted by the ankle orthosis, generating the corresponding motor torque. With this control architecture, it is intended that if the user performs (i) an ankle joint angle and torque trajectories closer to the references, the assistance of the ankle orthosis should be minimal; (ii) an ankle joint angle and/or torque trajectories different from the references, the ankle orthosis should provide assistance in order to compensate for these differences.

D. Experimental Procedures

Two experimental procedures were conducted to analyze (i) the robustness of the MVC computation; and (ii) the feasibility of the proposed AAN EMG-based control strategy.

Participant: One healthy participant (age: 27 years; body mass: 81.0 kg; body height: 1.70 m) without evidence of motor disorders accepted to participate in the study by signing a consent form according to the University of Minho Ethics Committee (CEICVS 006/2020).

MVC Computation Protocol: We carried out an experimental test to infer the robustness of the MVC computation algorithm in the presence of different perturbations. For that, a single EMG sensor was placed above the right *Tibialis Anterior* muscle of the participant. The participant lay on a stretcher, in a dorsal decubitus. The foot was manually immobilized while instructing the participant to execute two MVCs of the ankle dorsiflexion for 3 seconds each. During the first MVC, the EMG sensor was externally disturbed with a small hit. Between the first and the second MVCs, the EMG sensor was externally disturbed with various small hits with different magnitudes. The main goal of these hits is to generate external noise (generally, high peaks) in the EMG sensor acquisition, in order to see if the MVC algorithm is able to reject the high values associated with external hits.

Control Validation Protocol: To evaluate the effectiveness of the proposed AAN EMG-based control strategy, we started by collecting the participant's gender, age, body height and mass, and foot and shank lengths. Then, we instrumented the participant with (i) two EMG sensors placed on the right *Tibialis Anterior* and the right *Gastrocnemius Lateralis* muscles, following the SENIAM recommendations [30]; and (ii) 2 inertial measurement units (IMUs) from the InertialLab system (Fig. 1) [23], positioned in the pelvis and in the right thigh, to collect hip joint angles. Once instrumented with the sensor systems, the participant performed two MVCs per muscle. After that, the participant was instrumented with the SmartOs system (Fig. 3).

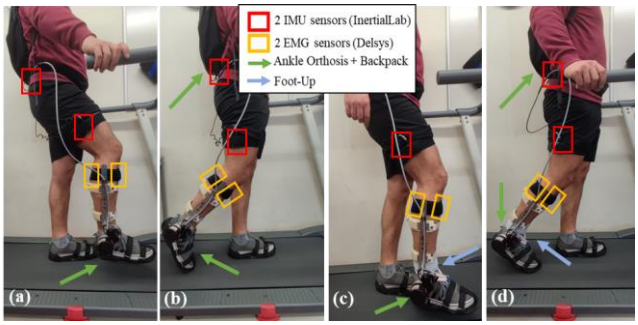

Fig. 3. Male participant equipped with the InertialLab, Delsys, and SmartOs systems (a) without the foot-up and with the right leg suspended; (b) without the foot-up and walking; (c) with the foot-up and with the right leg suspended; (d) with the foot-up and walking.

The experimental data acquisition was divided into two sessions, including three trials per session. For each trial of both sessions, the participant remained in the standing position with the right leg raised (without making any movement) for 30 s, followed by the walking motion on a treadmill at 1.0 km/h for 2 minutes. In the first session, the participant stood with the right leg raised (Fig. 3 – a)) and then, walked without any constraint at the right ankle joint (Fig. 3 – b). In the second session, this joint was conditioned, limiting the plantar flexion movement that the participant would be able to perform. This motion restriction was imposed by a foot-up, as illustrated in Fig. 3 – c) and Fig. 3 – d). Due to the inelastic characteristic of the foot-up, at the push-off phase of the gait cycle where the *Tibialis Anterior* is relaxed, the participant performed a small plantar flexion movement (around 0º) (Fig. 3 – d)), when compared to the condition without wearing a foot-up (Fig. 3 – b)). Consequently, it is expected a reduced Human ankle torque ($\tau_{meas.h}$) that should be compensated by increasing the orthosis motor torque.

III. Results and Discussion

A. MVC Algorithm

The complete trial with two MVCs is depicted in Fig. 4 – a). It shows (i) the first MVC with a disturbance (left) due to an external small hit performed; (ii) several disturbances due to various external small hits (middle) performed between 1st and 2nd MVCs; and (iii) the second MVC without disturbances, i.e., a valid MVC (right). As can be observed in Fig. 4 – b), every time that the average value of the horizontal window exceeds the average value of the vertical window, the peak is rejected, advancing to the next one. Fig. 4 – c) depicts the obtained MVC value.

B. AAN EMG-based Control

To analyze the contributions of the proposed AAN EMG-based control strategy, we analyzed the EMG signals of the *Tibialis Anterior* and *Gastrocnemius Lateralis*, the Human hip joint angle, the Human ankle joint torque, the motor torque, and the Human ankle joint angle in both conditions, i.e., with and without foot-up. For each variable, the mean value of the three trials was performed, as illustrated in Fig. 5. Fig. 5 – a) and Fig. 5 – b) present the variables' evolution during the standing position and walking motion, respectively, while the proposed AAN EMG-based control strategy was operating.

Tibialis Anterior and Gastrocnemius Lateralis EMG Analysis: From the results, we verified that during the standing position (Fig. 5 – a)), the EMG signals were close to 0%, representing that the user stayed with the right muscles relaxed during the standing. Contrarily, the EMG signals of both muscles increased when the participant performed the walking motion, even with and without foot-up (Fig. 5 – b)). During the walking motion, the foot-up use decreased on average (i) 41% of the *Gastrocnemius Lateralis* peak signals; and (ii) 29% of the *Tibialis Anterior* peak signals. These results are in line with what was expected. On one hand, the foot-up ensures by default a dorsiflexion movement; thus, the Human decreases the *Tibialis Anterior* muscle activation. On the other hand, the foot-up restricts the Human mobility to perform the plantar flexion movement; thus, the *Gastrocnemius Lateralis* muscle activation when using the foot-up is representatively lower.

Human Hip Joint Angle Analysis: As expected, the Human hip joint angles were constant during the standing phase and varied during the walking motion. During the standing phase (Fig. 5 – a)), lower hip angle values were recorded when using the foot-up, indicating that the participant flexed the hip less compared to when not using the foot-up. During the walking motion (Fig. 5 – b)) with foot-up, the participant (i) flexed the hip 14% more; and (ii) extended the hip 3% less, than the walking motion without foot-up.

Human Ankle Joint Torque Analysis: The Human ankle joint torque ($\tau_{meas.h}$) was estimated by the HTE block. While the anthropometric, and demographic data remained with fixed values, the EMG signals and the Human hip joint kinematics were measured in real-time.

Considering the results of Fig. 5 – a), the Human ankle joint torques were constant throughout the standing phase similar to the EMG signals and the Human hip joint angle. The low torque values estimated when using the foot-up are related to the lower Human hip joint angles when compared to not using the foot-up.

Additionally, the results of the walking motion (Fig. 5 – b)) revealed a decrease of 6 % in the peak ankle plantar flexion torque, when using the foot-up. These results are within what would be expected since the foot-up does not allow the human to perform as much plantar flexion torque compared to the condition without the foot-up. These findings demonstrate the foot-up efficacy in mimicking a condition of decreased Human joint torque that needed to be compensated by the ankle orthosis, as demonstrated in the following topic.

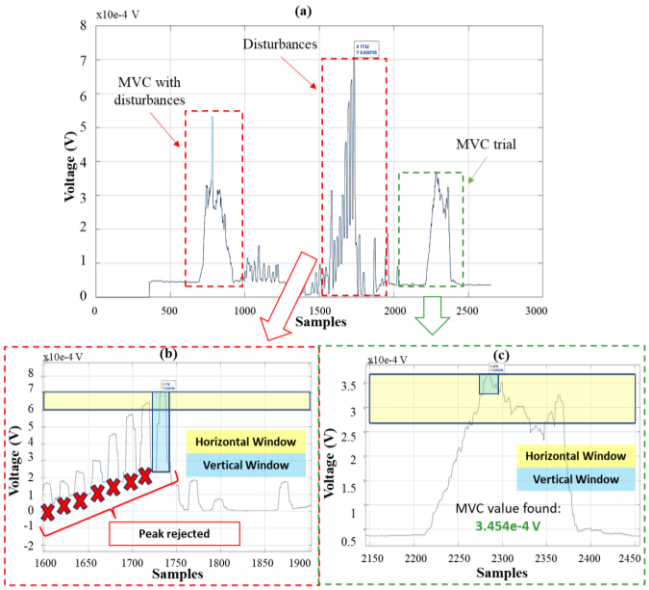

Fig. 4. MVC algorithm explanation. (a) trial with 2 MVCs; (b) an example of an unreliable maximum value; and (c) an example of a valid maximum value.

Motor Torque and Ankle Joint Angle Analysis: The motor torque represents the contribution of the ankle orthosis to perform the desired motion (in this case, the walking motion). As previously analyzed, during the standing phase (Fig. 5 – a)), the participant did not actively participate in the execution of the walking motion. Consequently, his EMG signals were close to the minimum values, which resulted in a constant and lower human ankle torque. Thus, the ankle orthosis is expected to be responsible for the execution of the walking motion. This can be proven by the motor torque and Human ankle joint torque trajectories presented in Fig. 5 – a). Since the participant was not performing the walking motion, the ankle orthosis generated the required motor torque to follow the reference ankle joint angle ($\Theta_{ref.o}$).

Moreover, considering that the foot-up decreased the plantar flexion (Human ankle plantar flexion torque decreased by 6 %) and supports the dorsiflexion movements of the ankle joint, it is expected that the ankle orthosis provides more assistance during plantar flexion phases and less assistance during dorsiflexion phases of the walking motion. According to the results obtained during the walking motion (Fig. 5 – b)), the foot-up usage resulted in (i) an increase of 28% in the plantar flexion motor torque; and (ii) a decrease of 18% in the dorsiflexion motor torque. These results show that the orthosis assisted as expected, indicating that it adapted its assistance in accordance with the user's participation while following the reference ankle joint angle ($\Theta_{ref.o}$).

D. Overall Analysis of the AAN EMG-based Control Strategy

This study was developed in the context of robotic gait rehabilitation, in which AAN EMG-based control strategies are needed to provide assistance training that invokes the user's participation while simultaneously providing assistance only when and as much as needed.

This study presents a proof-of-concept of an AAN EMG-based control strategy targeting ankle joint assistance, providing three key advances upon the state of the art. It proposes an automatic and real-time control strategy that (i) estimates the user's ankle joint torque in less than 2 ms without depending on complex, user-dependent calibration, and time-consuming methods [4], [15]–[18]; (ii) defines the desired user-oriented ankle joint torque trajectories, not relying on fixed assistance ratios [4], [15], [16]; and (iii) provides assistance during the entire gait cycle when and as much as required [4], [9], [16]–[18].

The achieved results indicate that the assistance of the ankle orthosis is automatically adjusted considering the user's participation. From the results, it was inferred that when the user revealed fewer muscle contributions (*Gastrocnemius Lateralis* and *Tibialis Anterior* less activated about 41% and 29%, respectively)), the Human ankle joint torque decreased by around 6% (foot-up condition). Consequently, the assistance of the ankle orthosis increased by 28%, which was demonstrated by the increase of the motor torque. In addition, the opposite was also verified, i.e., the ankle orthosis assistance decreased as the participant became more active (non-foot-up condition).

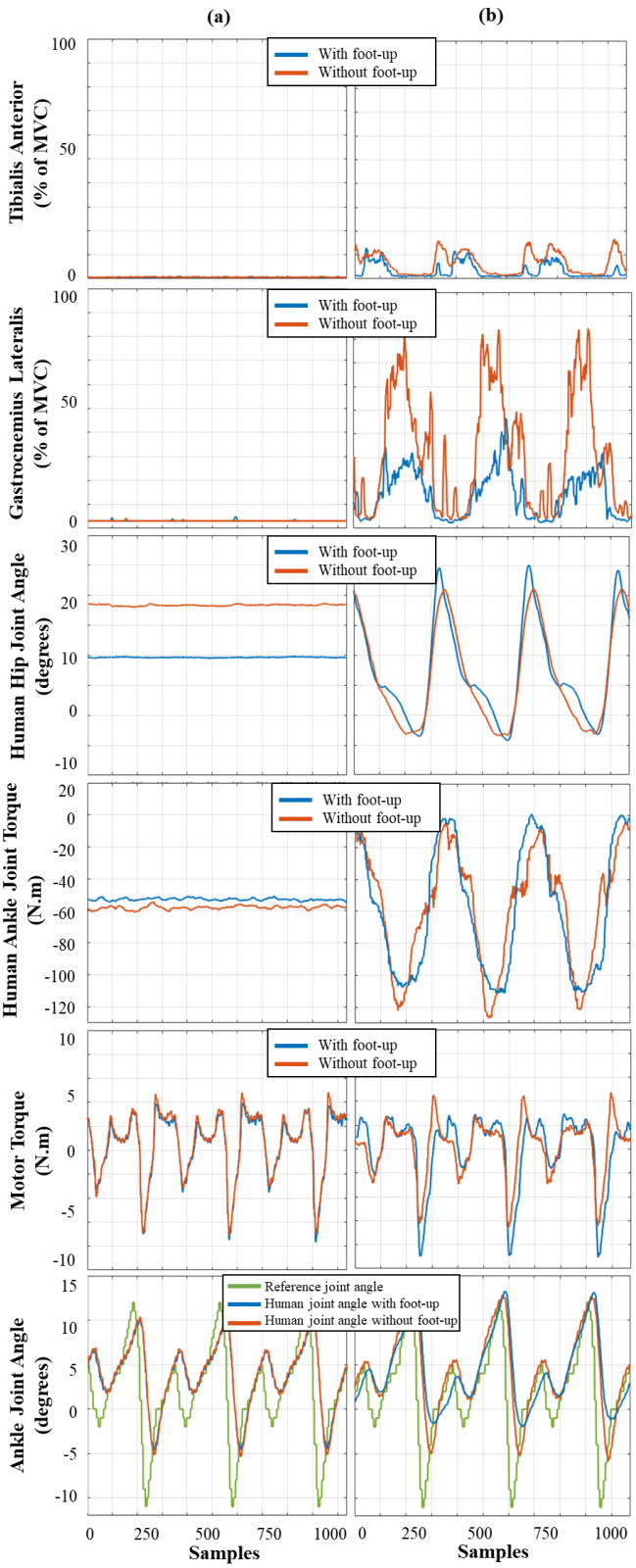

Fig. 5. Average trials of the two tested conditions: with foot-up (blue color) and without foot-up (orange color). Representation of the *Tibialis Anterior* signals, *Gastrocnemius Lateralis* signals, Human hip joint angles, Human ankle joint torques, motor torque, and ankle joint angles during the (a) standing position with the right leg raised; and (b) walking motion.

Despite the proposed AAN EMG-based control strategy offering promising results, there is still room for

improvement. This work used an inelastic foot-up to visualize if the proposed control strategy can increase its contribution (motor torque) when the user does not perform the gait pattern. The use of an inelastic foot-up may affect the achieved results. Although the ankle orthosis increased its contribution, the plantar flexion movement could not be completely performed due to the inelastic nature of the foot-up. Moreover, it is required to validate the proposed control strategy with more healthy participants and evaluate its impact on patients with lower limb impairments.

IV. Conclusions

This study addresses a gap in the current literature by proposing an AAN EMG-based control strategy to automatically assist the ankle joint throughout gait according to the user's disability level evaluated by EMG signals. The experimental results showed that the assistance of the ankle orthosis was automatically adapted according to the participant's involvement during the entire gait cycle. The orthosis increased the motor torque under decreased muscle activation, and vice-versa. Further studies would also involve more subjects, both healthy and pathological ones, to evaluate potential applications in ankle rehabilitation.

References

[1] W. Meng, Q. Liu, Z. Zhou, Q. Ai, B. Sheng, and S. S. Xie, "Recent development of mechanisms and control strategies for robot-assisted lower limb rehabilitation," *Mechatronics*, vol. 31, pp. 132–145, Oct. 2015, doi: 10.1016/j.mechatronics.2015.04.005.

[2] J. Zhang, C. C. Cheah, and S. H. Collins, "Torque Control in Legged Locomotion," in *Bioinspired Legged Locomotion*, 1st ed., Elsevier, 2017, pp. 347–400.

[3] S. Dalla Gasperina, L. Roveda, A. Pedrocchi, F. Braghin, and M. Gandolla, "Review on Patient-Cooperative Control Strategies for Upper-Limb Rehabilitation Exoskeletons," *Front. Robot. AI*, vol. 8, no. December, pp. 1–24, Dec. 2021, doi: 10.3389/frobt.2021.745018.

[4] K. Gui, U.-X. Tan, H. Liu, and D. Zhang, "Electromyography-Driven Progressive Assist-as-Needed Control for Lower Limb Exoskeleton," *IEEE Trans. Med. Robot. Bionics*, vol. 2, no. 1, pp. 50–58, Feb. 2020, doi: 10.1109/TMRB.2020.2970222.

[5] R. Baud, A. R. Manzoori, A. Ijspeert, and M. Bouri, "Review of control strategies for lower-limb exoskeletons to assist gait," *J. Neuroeng. Rehabil.*, vol. 18, no. 1, p. 119, Dec. 2021, doi: 10.1186/s12984-021-00906-3.

[6] H. I. Krebs *et al.*, "Rehabilitation robotics: Performance-based progressive robot-assisted therapy," *Auton. Robots*, vol. 15, no. 1, pp. 7–20, 2003, doi: 10.1023/A:1024494031121.

[7] L. Grazi, S. Crea, A. Parri, R. Molino Lova, S. Micera, and N. Vitiello, "Gastrocnemius Myoelectric Control of a Robotic Hip Exoskeleton Can Reduce the User's Lower-Limb Muscle Activities at Push Off," *Front. Neurosci.*, vol. 12, no. FEB, pp. 1–11, Feb. 2018, doi: 10.3389/fnins.2018.00071.

[8] A. Nasr, B. Laschowski, and J. McPhee, "Myoelectric Control of Robotic Leg Prostheses and Exoskeletons: A Review," in *Volume 8A: 45th Mechanisms and Robotics Conference (MR)*, Aug. 2021, pp. 1–8, doi: 10.1115/DETC2021-69203.

[9] R. Yang, Z. Shen, Y. Lyu, Y. Zhuang, L. Li, and R. Song, "Voluntary Assist-as-Needed Controller for an Ankle Power-Assist Rehabilitation Robot," *IEEE Trans. Biomed. Eng.*, vol. 70, no. 6, pp. 1795–1803, Jun. 2023, doi: 10.1109/TBME.2022.3228070.

[10] D. P. Ferris and C. L. Lewis, "Robotic lower limb exoskeletons using proportional myoelectric control," in *2009 Annual International Conference of the IEEE Engineering in Medicine and Biology Society*, Sep. 2009, pp. 2119–2124, doi: 10.1109/IEMBS.2009.5333984.

[11] S.-H. Yeo, J. Verheul, W. Herzog, and S. Sueda, "Numerical instability of Hill-type muscle models," *J. R. Soc. Interface*, vol. 20, no. 199, Feb. 2023, doi: 10.1098/rsif.2022.0430.

[12] T. Teramae, T. Noda, and J. Morimoto, "EMG-Based Model Predictive Control for Physical Human–Robot Interaction: Application for Assist-As-Needed Control," *IEEE Robot. Autom. Lett.*, vol. 3, no. 1, pp. 210–217, Jan. 2018, doi: 10.1109/LRA.2017.2737478.

[13] N. Li *et al.*, "Multi-Sensor Fusion-Based Mirror Adaptive Assist-as-Needed Control Strategy of a Soft Exoskeleton for Upper Limb Rehabilitation," *IEEE Trans. Autom. Sci. Eng.*, vol. 21, no. 1, pp. 475–487, Jan. 2024, doi: 10.1109/TASE.2022.3225727.

[14] J. C. Castiblanco, I. F. Mondragon, C. Alvarado-Rojas, and J. D. Colorado, "Assist-As-Needed Exoskeleton for Hand Joint Rehabilitation Based on Muscle Effort Detection," *Sensors*, vol. 21, no. 13, p. 4372, Jun. 2021, doi: 10.3390/s21134372.

[15] C. Fleischer and G. Hommel, "A Human-Exoskeleton Interface Utilizing Electromyography," *IEEE Trans. Robot.*, vol. 24, no. 4, pp. 872–882, Aug. 2008, doi: 10.1109/TRO.2008.926860.

[16] C. Caulcrick, W. Huo, E. Franco, S. Mohammed, W. Hoult, and R. Vaidyanathan, "Model Predictive Control for Human-Centred Lower Limb Robotic Assistance," *IEEE Trans. Med. Robot. Bionics*, vol. 3, no. 4, pp. 980–991, Nov. 2021, doi: 10.1109/TMRB.2021.3105141.

[17] Y. Zhu, Q. Wu, B. Chen, Z. Zhao, and C. Liang, "Physical Human–Robot Interaction Control of Variable Stiffness Exoskeleton With sEMG-Based Torque Estimation," *IEEE Trans. Ind. Informatics*, vol. 19, no. 10, pp. 10601–10612, Oct. 2023, doi: 10.1109/TII.2023.3240749.

[18] J. Xu *et al.*, "A Multi-Mode Rehabilitation Robot With Magnetorheological Actuators Based on Human Motion Intention Estimation," *IEEE Trans. Neural Syst. Rehabil. Eng.*, vol. 27, no. 10, pp. 2216–2228, Oct. 2019, doi: 10.1109/TNSRE.2019.2937000.

[19] L. Moreira, J. Figueiredo, J. P. Vilas-Boas, and C. P. Santos, "Kinematics, Speed, and Anthropometry-Based Ankle Joint Torque Estimation: A Deep Learning Regression Approach," *Machines*, vol. 9, no. 8, p. 154, Aug. 2021, doi: 10.3390/machines9080154.

[20] L. Moreira, R. M. Barbosa, J. Figueiredo, P. Fonseca, J. P. Vilas-Boas, and C. P. Santos, "Real-Time Torque Estimation Using Human and Sensor Data Fusion for Exoskeleton Assistance," in *The Sixth Iberian Robotics Conference - ROBOT2023*, 2024, pp. 450–461.

[21] J. Sofia Campos Figueiredo, "Smart Wearable Orthosis to Assist Impaired Human Walking," University of Minho, 2019.

[22] M. R. Tucker *et al.*, "Control strategies for active lower extremity prosthetics and orthotics: a review," *J. Neuroeng. Rehabil.*, vol. 12, no. 1, 2015, doi: 10.1186/1743-0003-12-1.

[23] J. Figueiredo, S. Carvalho, J. P. Vilas-Boas, L. M. Gonçalves, J. C. Moreno, and C. P. Santos, "Wearable Inertial Sensor System towards Daily Human Kinematic Gait Analysis : Benchmarking Analysis to MVN BIOMECH," *Sensors*, 2020, doi: 10.3390/s20082185.

[24] J. Figueiredo, C. Ferreira, L. Costa, L. P. Reis, J. C. Moreno, and C. P. Santos, "Instrumented Insole System for Ambulatory and Robotic Walking Assistance : First Advances," 2017.

[25] Delsys Incorporated, "TRIGNO ® Wireless System SDK User's Guide." pp. 1–29, 2019, [Online]. Available: https://www.delsys.com/downloads/USERSGUIDE/trigno/sdk.pdf.

[26] M. Bortole *et al.*, "The H2 robotic exoskeleton for gait rehabilitation after stroke: early findings from a clinical study," *J. Neuroeng. Rehabil.*, vol. 12, no. 1, p. 54, Dec. 2015, doi: 10.1186/s12984-015-0048-y.

[27] D. Meldrum, E. Cahalane, R. Conroy, D. Fitzgerald, and O. Hardiman, "Maximum voluntary isometric contraction: Reference values and clinical application," *Amyotroph. Lateral Scler.*, vol. 8, no. 1, pp. 47–55, Jan. 2007, doi: 10.1080/17482960601012491.

[28] B. Koopman, E. H. F. van Asseldonk, and H. van der Kooij, "Speed-dependent reference joint trajectory generation for robotic gait support," *J. Biomech.*, vol. 47, no. 6, pp. 1447–1458, 2014, doi: 10.1016/j.jbiomech.2014.01.037.

[29] P. Félix, J. Figueiredo, C. P. Santos, and J. C. Moreno, "Electronic design and validation of powered knee orthosis system embedded with wearable sensors," *17th Int. Conf. Auton. Robot Syst. Compet.*, 2017.

[30] H. J. Hermens, B. Freriks, C. Disselhorst-Klug, and G. Rau, "Development of recommendations for SEMG sensors and sensor placement procedures," *J. Electromyogr. Kinesiol.*, vol. 10, pp. 361–374, 2000, doi: 10.1007/s10750-015-2551-3.